

# Novel Extraction Method of Inductance Parameter for Nonuniform Transmission Line in Anisotropic Dielectric

Yaxiu Sun and Xiaomeng Wang

College of Information and Communication Engineering  
Harbin Engineering University, Harbin, 150001, China  
sunyaxiu@hrbeu.edu.cn, wangxiaomeng@hrbeu.edu.cn

**Abstract** — Since the parameters of transmission line can affect the signal integrity and electromagnetic compatibility directly in high frequency circuit, and there is lack of researches in the field of solving the inductance parameter of nonuniform transmission line in anisotropic dielectric, a novel method has been proposed in this paper to solve this problem. The new method uses filament division to establish the dispersion model of nonuniform transmission line, and formulates the filament division principle based on Biot-Savart Law and skin effect. Then it develops the Ampere loop integral dyadic equations and the closed circuit dyadic impedance matrix equation with direction factor in frequency domain based on electromagnetic quasi-static (EMQS). To obtain the corresponding magnetic field direction factor, the relative position of filaments in geometric space is analyzed. Finally, the inductance parameters are obtained by the impedance matrix equation. The correctness of proposed method is verified by applying to uniform transmission line model. Then the new method is applied to the calculation of two nonuniform transmission line models which filled in free space and anisotropic dielectric respectively. The inductance parameters and frequency dependency solved by different methods are compared, showing accuracy and validity of the proposed method. Besides, the new method can be applied to various transmission line structures and different anisotropic dielectric.

**Index Terms** — Anisotropic dielectric, inductance parameter, nonuniform transmission line, tensor dielectric constant.

## I. INTRODUCTION

Nonuniform transmission line has been widely used in high speed circuit systems and affected the circuit performance and reliability [1-4]. So the extraction of distributed parameter for nonuniform transmission line is particularly important. Many electromagnetic numerical methods have been extensively used to solve this problem, such as finite-difference time-domain (FDTD) and moment of method (MOM) [5-9]. Afroz and his

fellows have used FDTD to analyze the electromagnetic field and extract the inductance parameter from the time-domain difference transmission line equations [5]. However, it cannot take the skin effect into consideration when current is in high frequency, so that the parameter value is inaccurate. Paul extracted the capacitance matrix by using MoM, and then the inductance matrix can be obtained from it [8]. Although this method can effectively solve the inductance matrix of transmission line, the analysis process is complex and needs to be solved many times. For this problem, the researchers of MIT have developed a FastHenry software to extract the parameters of integrated circuit based on the network analysis method. This software can solve the parameter fast, exactly, and universally. However, this software can be invalidated when the circuits are under the condition of electromagnetic quasi-static (EMQS) [10]. Besides, with the development of engineering technology, the performance of the circuit filled in general medium can no longer meet the demand of circuit design. So anisotropic dielectric has been more widely used because of the special electromagnetic characteristics [11-13]. For the research of anisotropic dielectric, many achievements focus on the influence of electromagnetic wave radiation, while few researches focus on inductance extraction of nonuniform transmission line in anisotropic dielectric [14-15].

In this paper, a novel extraction method of inductance parameters for nonuniform transmission line in anisotropic dielectric is proposed. It establishes the filament physical model according to Biot-Savart Law and skin effect, and derives the Ampere circuit dyadic integral equations and closed circuit dyadic impedance matrix equation with direction factor in frequency domain. Finally, the inductance parameter can be solved. The new method can be applied to various complex nonuniform transmission line structures and has some theoretical significance and engineering value.

This paper is organized as follows. In Section II, the filament dispersion of nonuniform transmission line is introduced and Ampere loop integral dyadic equations are summarized. The closed circuit dyadic impedance

matrix equation with direction factor is obtained in Section III. The proposed method is finally verified by numerical examples in Section IV, showing the correctness, accuracy and validity. The conclusions are given in Section V.

## II. NONUNIFORM TRANSMISSION LINE MODELING

### A. Filament division of nonuniform transmission line model

A physical structure is established and shown in Fig. 1 to solve the inductance parameter of nonuniform transmission line. It consists of a lossy nonuniform signal line and a ground plate. The direction of signal line is Z. Its section radius is  $r(z)$ .

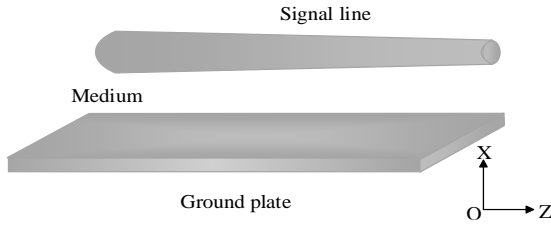


Fig. 1. The nonuniform transmission line model.

The structure in Fig. 1 can be discretized into some filaments with an approximate cross section. The number of filaments can be determined based on skin effect and the filament condition of Biot-Savart Law. So the side length of filament section  $g$  should meet the condition:

$$g \leq \frac{1}{5} \delta, \quad (1)$$

where skin depth  $\delta$  can be described as  $\delta = 1 / \sqrt{\pi f \mu \sigma}$ .  $f$  is frequency,  $\mu$  is permeability,  $\sigma$  is conductivity. So filament number  $N$  should meet the condition:

$$N \geq \frac{s(z)}{g^2}, \quad (2)$$

where  $s(z)$  is the effective section which is described as:

$$s(z) = \pi \left[ r(z)^2 - [r(z) - \delta]^2 \right] = \pi \delta^2 + 2\pi r(z)\delta, \delta < r(z). \quad (3)$$

When the frequency is enough high,  $s(z)$  can be approximately described as:

$$s(z) = 2\pi r(z)\delta = 2r(z) \cdot \sqrt{\pi / f \mu \sigma}, \delta \ll r(z). \quad (4)$$

The final update equation can be written as:

$$N \geq 50\pi r(z) \sqrt{\pi f \mu \sigma}. \quad (5)$$

Equation (5) is the condition of the filament division.

According to the condition of filament division, the model in Fig. 1 is discretized as Fig. 2. The filament numbers of signal line and ground plate are  $N_C$  and  $N_D$ . The total filament number is  $N_{\text{tot}}$ . When the section of filament is small enough, it can be considered that the current here is evenly distributed. So the current of

filament  $n$  at  $z$  point can be expressed as  $i_n(z) = J_n(z)S_0$ , where  $J_n(z)$  is the current density of filament  $n$  at  $z$  point,  $S_0$  is the area of filament section.

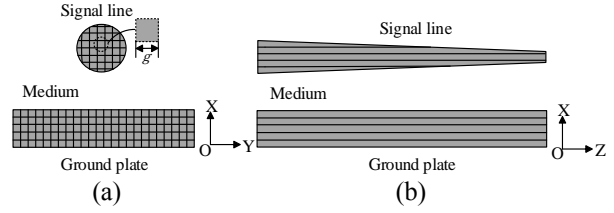


Fig. 2. Filament division of nonuniform transmission line: (a) XOY plane and (b) XOZ plane.

### B. Filaments circuit modeling

Figure 3 is the instruction of filaments circuit  $a \rightarrow b \rightarrow c \rightarrow d \rightarrow a$ , in which the filaments  $k$  and  $s$  are chosen any from the filaments of signal line and ground plate. The length of filament is  $\Delta z$ . The circuit is in Electromagnetic quasi-static (EMQS).

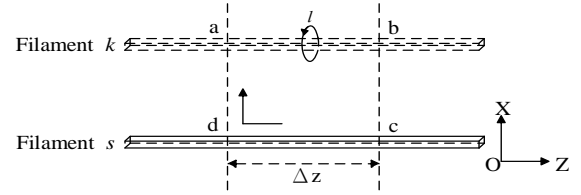


Fig. 3. The instruction of filaments circuit.

According to Faraday electromagnetic law, the closed circuit integral equation in frequency domain can be written as:

$$\begin{aligned} & \int_a^b \mathbf{E}_k(x, y, z) dz + \int_b^c \mathbf{E}(x, y, z + \Delta z) dx \\ & + \int_c^d \mathbf{E}_s(x, y, z) dz + \int_d^a \mathbf{E}(x, y, z) dx \\ & = -j\omega\mu \int_s^{z+\Delta z} \mathbf{H}_\perp(x, y, z) dz dx. \end{aligned} \quad (6)$$

The left part of (6) can be expressed as:

$$\int_a^b \mathbf{E}_k(x, y, z) dz = i_k(z) R_k \Delta z, \quad (7)$$

$$\int_b^c \mathbf{E}(x, y, z + \Delta z) dx = v_k(z + \Delta z) - v_s(z + \Delta z), \quad (8)$$

$$\int_c^d \mathbf{E}_s(x, y, z) dz = -i_s(z) R_s \Delta z, \quad (9)$$

$$\int_d^a \mathbf{E}(x, y, z) dx = v_s(z) - v_k(z), \quad (10)$$

where  $\mathbf{E}(x, y, z)$  is spatial electric field strength;  $\mathbf{E}_k(x, y, z)$  and  $\mathbf{E}_s(x, y, z)$  are electric field strength of filaments  $k$  and  $s$  respectively;  $v_k(z)$  and  $v_s(z)$  are the voltage of filaments  $k$  and  $s$  at point  $z$ ;  $R_k$  and  $R_s$  are the unit resistance of filaments  $k$  and  $s$ .

The right part of (6) can be described as follows:

$$\mu \int_s^k \int_z^{z+\Delta z} \mathbf{H}_{n\perp}(x, y, z) dz dx = \mu \sum_{n=1}^{N_{tot}} \int_s^k \int_z^{z+\Delta z} \mathbf{H}_{n\perp}(x, y, z) dz dx, \quad (11)$$

where  $\mathbf{H}_{n\perp}(x, y, z)$  is the magnetic field component of filament  $n$  which vertically through the area of  $a \rightarrow b \rightarrow c \rightarrow d \rightarrow a$ .

So the Equation (6) can be updated as:

$$\begin{aligned} & v_k(z + \Delta z) - v_k(z) - v_s(z + \Delta z) \\ & + v_s(z) + i_k(z) R_k \Delta z - i_s(z) R_s \Delta z \\ & = -j\omega\mu \sum_{n=1}^{N_{tot}} \int_s^k \int_z^{z+\Delta z} \mathbf{H}_{n\perp}(x, y, z) dz dx. \end{aligned} \quad (12)$$

Taking the filament  $k$  as an example, the Ampere loop integral equation can be written as:

$$\oint \mathbf{H}_k \cdot d\mathbf{l} = \int_s \mathbf{J}_k \cdot d\mathbf{s} + j\omega \int_s \mathbf{D}_k \cdot d\mathbf{s}, \quad (13)$$

where  $\mathbf{H}_k$  is total magnetic field strength of filament  $k$  through the area of  $a \rightarrow b \rightarrow c \rightarrow d \rightarrow a$ ,  $\mathbf{J}_k$  and  $\mathbf{D}_k$  are the conduction current density and electric displacement vector respectively, where  $\mathbf{J}_k$  can be expressed as  $\mathbf{J}_k = \sigma \mathbf{E}$ .

### C. Ampere loop integral dyadic equations

The constitutive relation of isotropic medium is only simple one dimension relationship which can be represented as  $\mathbf{D} = \varepsilon \mathbf{E}$ . However, it usually takes anisotropic dielectric as medium in application. The dielectric constant  $\varepsilon$  of anisotropic dielectric shows a form of tensor, and it can be described as a matrix:

$$[\varepsilon_{ki}] = \begin{bmatrix} \varepsilon_{11} & \varepsilon_{12} & \varepsilon_{13} \\ \varepsilon_{21} & \varepsilon_{22} & \varepsilon_{23} \\ \varepsilon_{31} & \varepsilon_{32} & \varepsilon_{33} \end{bmatrix}. \quad (14)$$

So the constitutive relations of anisotropic dielectric can be written as follows:

$$\mathbf{D}_k = \sum_{i=1}^3 \varepsilon_{ki} \mathbf{E}_i \quad (k=1,2,3), \quad (15)$$

and it can also be represented in dyadic form as:

$$\mathbf{D} = \overset{=}{\varepsilon} \mathbf{E}, \quad (16)$$

where  $\overset{=}{\varepsilon}$  is the dielectric constant tensor.

In this paper, the electric anisotropic dielectric is taken as the example, whose three principal axes coincide with the coordinate axes and the dielectric constant tensor is symmetric. So the dielectric constant tensor can be written as:

$$\overset{=}{\varepsilon} = \begin{bmatrix} \varepsilon_{11} & 0 & 0 \\ 0 & \varepsilon_{22} & 0 \\ 0 & 0 & \varepsilon_{33} \end{bmatrix}. \quad (17)$$

By applying the new constitutive relations to (13), the following expression can be obtained as:

$$\int_s \mathbf{J}_k \cdot d\mathbf{s} + j\omega \int_s \mathbf{D}_k \cdot d\mathbf{s} = \int_s \sigma \mathbf{E}_k \cdot d\mathbf{s} + j\omega \int_s (\overset{=}{\varepsilon} \cdot \mathbf{E}_k) \cdot d\mathbf{s}, \quad (18)$$

which leads to:

$$\int_s \mathbf{J}_k \cdot d\mathbf{s} + j\omega \int_s \mathbf{D}_k \cdot d\mathbf{s} = j\omega \int_s \left( \frac{\overset{=}{\sigma} \mathbf{A}}{j\omega} + \overset{=}{\varepsilon} \right) \cdot d\mathbf{s}, \quad (19)$$

where  $\mathbf{A}$  is the unit matrix. So the right part of (19) can be further derived as:

$$j\omega \int_s \left( \frac{\overset{=}{\sigma} \mathbf{A}}{j\omega} + \overset{=}{\varepsilon} \right) \mathbf{E}_k \cdot d\mathbf{s} = j\omega \int_s \overset{=}{\zeta} \mathbf{E}_k \cdot d\mathbf{s}, \quad (20)$$

in which  $\overset{=}{\zeta} = \frac{\overset{=}{\sigma} \mathbf{A}}{j\omega} + \overset{=}{\varepsilon}$ . Then the Ampere loop integral

dyadic equation in frequency domain can be written as:

$$\oint_c \mathbf{H}_k \cdot d\mathbf{l} = j\omega \int_s \overset{=}{\zeta} \mathbf{E}_k \cdot d\mathbf{s}. \quad (21)$$

Therefore,  $\mathbf{H}_k$  can be solved by this equation. The magnetic field strengths  $\mathbf{H}_n$  produced by the other filaments can also be obtained by this equation. To obtain  $\mathbf{H}_{n\perp}$ , a new parameter has been defined here, that is the direction factor  $\beta$ . It shows the relationship between effective magnetic  $\mathbf{H}_{n\perp}$  and total magnetic  $\mathbf{H}_n$  through the particular rectangular loop. And this relationship cannot be expressed in simple mathematical expressions. The expression and usage of direction factor will be described in next section.

## III. FORMULATION OF CLOSED CIRCUIT DYADIC IMPEDENCE MATRIX EQUATION

### A. Expression of direction factor

Direction factor  $\beta$  can be solved according to the relative geometric position of filaments and rectangular loop. To solve the corresponding direction factor of  $\mathbf{H}_{n\perp}$ , the rectangular loop of filament  $k$  and  $s$  is taken as the example.

The section center point coordinates of filament  $k$ ,  $s$ , and  $n$  are  $(x_k, y_k)$ ,  $(x_s, y_s)$ , and  $(x_n, y_n)$ . The right part of (12) can be represented as:

$$\begin{aligned} & \mu \sum_{n=1}^{N_{tot}} \int_s^k \int_z^{z+\Delta z} \mathbf{H}_{n\perp} dz dx = \\ & \mu \int_s^k \int_z^{z+\Delta z} \mathbf{H}_{k\perp} dz dx + \mu \int_s^k \int_z^{z+\Delta z} \mathbf{H}_{s\perp} dz dx + \mu \sum_{n=1, n \neq k}^{N_{tot}} \int_s^k \int_z^{z+\Delta z} \mathbf{H}_{n\perp} dz dx, \end{aligned} \quad (22)$$

where  $\mu \int_s^k \int_z^{z+\Delta z} \mathbf{H}_{k\perp} dz dx$  and  $\mu \int_s^k \int_z^{z+\Delta z} \mathbf{H}_{s\perp} dz dx$  are the magnetic flux induced by the current of filaments  $k$  and  $s$ . Then they can be further derived as:

$$\begin{aligned} & \int_s^k \int_z^{z+\Delta z} \mathbf{H}_{k\perp} dz dx = -\frac{1}{8\pi} \frac{j\omega \overset{=}{\zeta}}{\sigma} i_k \Delta z - \int_0^c \int_b^c \mathbf{H}_{k\perp} dz dx \\ & = -\frac{1}{8\pi} \frac{j\omega \overset{=}{\zeta}}{\sigma} i_k \Delta z - \frac{1}{2\pi} \frac{j\omega \overset{=}{\zeta}}{\sigma} i_k \Delta z \ln \frac{\sqrt{(x_k - x_s)^2 + (y_k - y_s)^2} - g}{g}, \end{aligned} \quad (23)$$

$$\begin{aligned} & \int_s^k \int_z^{z+\Delta z} \mathbf{H}_{s\perp} dz dx \\ &= \frac{1}{8\pi} \frac{j\omega\zeta}{\sigma} i_s \Delta z + \frac{1}{2\pi} \frac{j\omega\zeta}{\sigma} i_s \Delta z \ln \frac{\sqrt{(x_k-x_s)^2+(y_k-y_s)^2}-g}{g}. \end{aligned} \quad (24)$$

The third part of (22) is the magnetic flux induced by the current of filaments except  $k$  and  $s$ , and can be written as:

$$\begin{aligned} & \sum_{n=1}^{N_{tot}} \int_s^k \int_z^{z+\Delta z} \mathbf{H}_{n\perp} dz dx = \sum_{n=1}^{N_{tot}} \int_s^k \int_z^{z+\Delta z} \mathbf{H}_n \cdot \beta dz dx \\ & \quad n \neq k, n \neq s \quad n \neq k, n \neq s \quad (25) \\ &= \sum_{n=1}^{N_{tot}} \int_0^{(x_k-x_s)^2+(y_k-y_s)^2} \int_z^{z+\Delta z} \mathbf{H}_n \cos \alpha dz dx, \\ & \quad n \neq k, n \neq s \end{aligned}$$

where  $\alpha$  is the angle between magnetic flux and rectangular loop of filaments  $k$  and  $s$ . Based on the multiple relative position among filaments  $k$ ,  $s$  and  $n$ , Equation (25) are final updated as:

$$\begin{aligned} & \sum_{n=1}^{N_{tot}} \int_s^k \int_z^{z+\Delta z} \mathbf{H}_{n\perp} dz dx \\ & \quad n \neq k, n \neq s \quad (26) \\ &= \sum_{n=1}^{N_{tot}} \frac{1}{4\pi} \frac{j\omega\zeta}{\sigma} i_n \Delta z \ln \frac{(u \cos \theta - v)^2 + (u \sin \theta)^2}{(u \cos \theta + v)^2 + (u \sin \theta)^2}, \\ & \quad n \neq k, n \neq s \end{aligned}$$

where

$$\begin{aligned} u &= \sqrt{\left(x_n - \frac{x_k+x_s}{2}\right)^2 + \left(y_n - \frac{y_k+y_s}{2}\right)^2}, \\ v &= \frac{\sqrt{(x_k-x_s)^2+(y_k-y_s)^2}}{2}, \\ w &= \sqrt{(x_k-x_n)^2+(y_k-y_n)^2}, \\ \cos \theta &= \frac{u^2+v^2-w^2}{2uv}. \end{aligned}$$

Therefore, the corresponding direction factor  $\beta$  of  $\mathbf{H}_{n\perp}$  has been simplified as a relationship between the filament section center point coordinates and angle  $\alpha$ . These variables can be obtained directly. So the corresponding direction factor can be represented as a relationship:

$$\beta = \frac{\sum_{n=1}^{N_{tot}} \int_s^k \int_z^{z+\Delta z} \mathbf{H}_{n\perp} dz dx}{\sum_{n=1}^{N_{tot}} \int_s^k \int_z^{z+\Delta z} \mathbf{H}_n dz dx} \quad n \neq k, n \neq s \quad (27)$$

The direction factor of other filaments can also be obtained based on above process.

### B. Closed circuit dyadic equations with direction factor

The total number of filament circuits is  $C_{N_{tot}}^2$ . They

are similar to the filaments circuit of  $k$  and  $s$ . Taking the convenience and realization for calculation into account, the closed circuits which constituted by all signal line filaments with the first filament (namely  $N_C+1$ ) of ground plate are selected. Moreover, the closed circuits constituted by all ground plate filaments with the longest one (namely filament  $k$ ) of signal line are selected too. So the closed circuit dyadic equations with direction factor can be concluded as follows:

when  $1 \leq m \leq N_C$ ,

$$\begin{aligned} & \frac{v_m(z+\Delta z) - v_m(z)}{\Delta z} \\ &= -\lambda'(i_m - i_{N_C+1}) + \frac{\omega^2 \mu}{\sigma} \zeta \sum_{n=1}^{N_{tot}} \frac{i_n}{4\pi} \ln \frac{(u' \cos \theta' - v')^2 + (u' \sin \theta')^2}{(u' \cos \theta' + v')^2 + (u' \sin \theta')^2}, \\ & \quad n \neq m, n \neq N_C+1 \end{aligned} \quad (28)$$

where

$$\begin{aligned} \lambda' &= \frac{1}{4\sigma g^2} \frac{\omega^2 \mu}{\sigma} \zeta \left[ \frac{1}{8\pi} + \frac{1}{2\pi} \ln \frac{\sqrt{(x_m-x_{N_C+1})^2+(y_m-y_{N_C+1})^2}-g}{g} \right], \\ u' &= \sqrt{\left(x_n - \frac{x_m+x_{N_C+1}}{2}\right)^2 + \left(y_n - \frac{y_m+y_{N_C+1}}{2}\right)^2}, \\ v' &= \frac{\sqrt{(x_m-x_{N_C+1})^2+(y_m-y_{N_C+1})^2}}{2}, \\ w' &= \sqrt{(x_m-x_n)^2+(y_m-y_n)^2}, \\ \cos \theta' &= \frac{u'^2+v'^2-w'^2}{2u'v'}. \end{aligned}$$

when  $N_C+1 \leq m \leq N_{tot}$ ,

$$\begin{aligned} & \frac{v_{N_k}(z+\Delta z) - v_{N_k}(z)}{\Delta z} \\ &= -\lambda''(i_{N_k} - i_m) + \frac{\omega^2 \mu}{\sigma} \zeta \sum_{n=1}^{N_{tot}} \frac{i_n}{4\pi} \ln \frac{(u'' \cos \theta'' + v'')^2 + (u'' \sin \theta'')^2}{(u'' \cos \theta'' - v'')^2 + (u'' \sin \theta'')^2}, \\ & \quad n \neq m, n \neq N_k \end{aligned} \quad (29)$$

where

$$\begin{aligned} \lambda'' &= \frac{1}{4\sigma g^2} \frac{\omega^2 \mu}{\sigma} \zeta \left[ \frac{1}{8\pi} + \frac{1}{2\pi} \ln \frac{\sqrt{(x_m-x_{N_k})^2+(y_m-y_{N_k})^2}-g}{g} \right], \\ u'' &= \sqrt{\left(x_n - \frac{x_m+x_{N_k}}{2}\right)^2 + \left(y_n - \frac{y_m+y_{N_k}}{2}\right)^2}, \\ v'' &= \frac{\sqrt{(x_m-x_{N_k})^2+(y_m-y_{N_k})^2}}{2}, \\ w'' &= \sqrt{(x_{N_k}-x_n)^2+(y_{N_k}-y_n)^2}, \\ \cos \theta'' &= \frac{u''^2+v''^2-w''^2}{2u''v''}. \end{aligned}$$

There is a duplicate closed circuit dyadic equation in above equations. So we should remove it and add the

current conservation equation which can be written as:

$$\sum_{n=1}^{N_{\text{tot}}} i_n = 0. \quad (30)$$

Therefore, there are  $N_{\text{tot}}$  equations totally.

### C. Matrix form of closed circuit dyadic equations

The voltage and current of signal line is  $V(z)$  and  $I(z)$ . The potential of ground plate is zero. When  $\Delta z \rightarrow 0$ , the closed circuit dyadic equations can be written in matrix form, and the current conservation equation can be added in the  $N_C+1$  row of the matrix.  $N_C$  can be obtained based on Equation (5). So the matrix form of the closed circuit equations is:

$$\mathbf{FD} = -\mathbf{SM} \quad (31)$$

where  $\mathbf{F}(m,1) = \begin{cases} 0, & m = N_C + 1 \\ 1, & \text{others} \end{cases}$ ,  $\mathbf{D} = \frac{dV(z)}{dz}$ .  $\mathbf{S}$  is

$N_{\text{tot}} \times N_{\text{tot}}$  coefficient matrix which can be obtained by the closed circuit equations and written as:

$$\mathbf{S}(m,n) = \begin{cases} \lambda', & 1 \leq m \leq N_C, 1 \leq n \leq N_{\text{tot}}, m = n \\ -\lambda', & 1 \leq m \leq N_C, n = N_C + 1 \\ -\frac{\omega^2 \mu}{4\pi\epsilon} \zeta \ln \frac{(u' \cos \theta' - v')^2 + (u' \sin \theta')^2}{(u' \cos \theta' + v')^2 + (u' \sin \theta')^2}, & 1 \leq m \leq N_C, 1 \leq n \leq N_{\text{tot}}, m \neq n \\ 1, & m = N_C + 1, 1 \leq n \leq N_{\text{tot}} \\ -\lambda'', & N_C + 2 \leq m \leq N_{\text{tot}}, 1 \leq n \leq N_{\text{tot}}, m = n \\ \lambda'', & N_C + 2 \leq m \leq N_{\text{tot}}, n = N_C \\ -\frac{\omega^2 \mu}{4\pi\epsilon} \zeta \ln \frac{(u'' \cos \theta'' + v'')^2 + (u'' \sin \theta'')^2}{(u'' \cos \theta'' - v'')^2 + (u'' \sin \theta'')^2}, & N_C + 2 \leq m \leq N_{\text{tot}}, 1 \leq n \leq N_{\text{tot}}, m \neq n \end{cases}$$

$\mathbf{M}$  is  $N_{\text{tot}} \times 1$  current matrix:

$$\mathbf{M} = (i_1 \ i_2 \ \cdots \ i_c \ i_{c+1} \ i_{c+2} \ \cdots \ i_{\text{tot}})^T.$$

Another relationship can be concluded as:

$$\mathbf{I}(z) = \mathbf{QM} \quad (32)$$

where  $\mathbf{Q}(1,m) = \begin{cases} 1, & 1 \leq m \leq N_C \\ 0, & \text{others} \end{cases}$ .

By applying the matrix transformation, the updated relationship can be written as:

$$\mathbf{D} = -(\mathbf{QS}^{-1}\mathbf{F})^{-1}\mathbf{I}(z) \quad (33)$$

This equation is the closed circuit impedance dyadic matrix equation with direction factor. Thus, the impedance matrix can be expressed as:

$$\mathbf{Z} = (\mathbf{QS}^{-1}\mathbf{F})^{-1} \quad (34)$$

According to the transmission line impedance equation  $\mathbf{Z} = \mathbf{R} + j\omega\mathbf{L}$ , the resistive parameter can be obtained from the real part of Equation (34), and the inductance matrix can also be concluded from the imaginary part as:

$$\mathbf{L}(z) = \frac{\text{Im}[\mathbf{Z}]}{2\pi f} = \frac{\text{Im}[(\mathbf{QS}^{-1}\mathbf{F})^{-1}]}{2\pi f} \quad (35)$$

## IV. NUMERICAL RESULTS

### A. Uniform transmission line model in free space

In this section, the uniform transmission line model shown in Fig. 4 is considered to verify the validity and

correctness of the new method. The two kind of different radius of signal line we used here are  $r_1=0.5$  mm and  $r_2=0.4$  mm. The size of cross section of ground plate is 3 mm×1 mm. The nearest distance between signal line and ground plate is 1 mm. The conductivity of transmission line is  $\sigma=5.98 \times 10^7$  S/m. The magnetic permeability is  $\mu = \mu_0$ . New method and traditional method are used to solve the inductance parameter of this model.

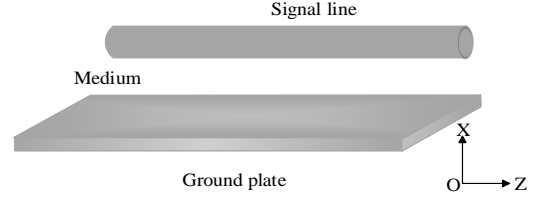


Fig. 4. The uniform transmission line model.

To verify the correctness of proposed method, the per unit length inductance of uniform transmission line has been obtained by three different methods: proposed method, traditional method and measurement. In traditional method, the skin effect of transmission line in high frequency has been neglected, which can decrease the area of effective cross section and affect the value of inductance parameter [16]. While the new method can take it into consideration. Besides, the measurement has also been used to prove the validity of proposed method. The schematic of measurement is shown in Fig. 5. It uses the vector network analyzer to measure the impedance of equipment under test (EUT), namely, the transmission line, and the inductance parameter can be obtained from it.

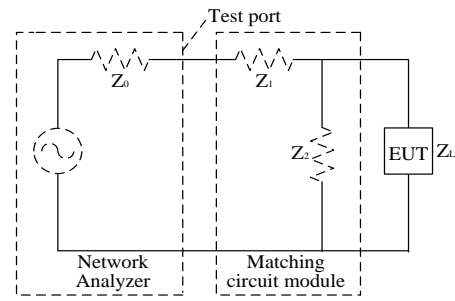


Fig. 5. Measurement setup schematic.

Table 1 shows the filament numbers and computing time of new method to calculate the inductance parameter in various frequency.

Figure 6 shows the inductance distribution of uniform transmission line in free space and 100 MHz frequency. As shown in the figure, we can conclude that the per unit length inductance does not change with the coordinate  $z$ . Moreover, the inductance values of the line

with different radius are different, and they increase with the decrease of radius when the frequency of current is constant. Compare the traditional method and the proposed method, the changing trend of the new method is more close to the measurement one. So the correctness of proposed method has been verified, and it is more accurate than traditional one.

The frequency dependency of inductance parameter for uniform transmission line is shown in Fig. 7, which indicates the inductance calculated by new method and the measurement are vary with frequency, while the traditional method does not. Because traditional method cannot consider the skin effect in high frequency. Besides, comparing the results with measurement, the error between new method and measurement is less than 5%, namely 15nH. So the validity and correctness of new method can be verified, and it has a high precision.

Table 1: Filament numbers and computing time in various frequency

$f/\text{MHz}$	$N_C$	$N_D$	$N_{\text{tot}}$	$t/\text{s}$
10	381	871	1252	0.52
100	1206	2972	4178	2.6
1000	3815	9615	13430	30.45

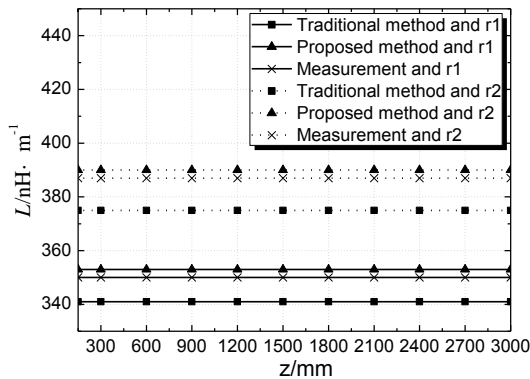


Fig. 6. Inductance distribution of uniform transmission line in free space.

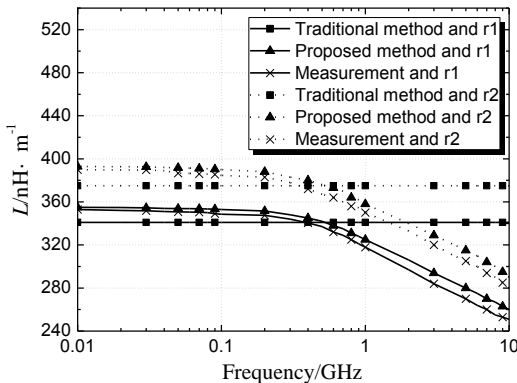


Fig. 7. Frequency dependency of inductance parameter for uniform transmission line.

In order to further illustrate the influence that the skin effect bring to the calculation of inductance parameter in high frequency, Fig. 8 shows the frequency dependency for unit inductance parameters expressed by the ratio of radius to skin depth. When the radius of conductor is less than twice the skin depth, the unit inductance parameter of new method is approximately equal to the value of traditional method (341nH/m). The reason is that the current can be considered as uniform distributed in low frequency. However, the radius of conductor is twice larger than skin depth, the unit inductance parameter is gradually decreased with the increased frequency. So the skin effect in high frequency cannot be ignored.

Figure 9 shows the current distribution within the cross section of the uniform transmission line at different frequency. It shows the variation of current density along the radial direction at 1 MHz, 10 MHz and 100 MHz frequency respectively. Compare the curves, we can further validate the effect of skin effect and get the conclusion; as the frequency increases, the skin depth of the wire decreases, and the smaller the effective area of the current along the wire. Thus, the greater the resistance loss of the wire.

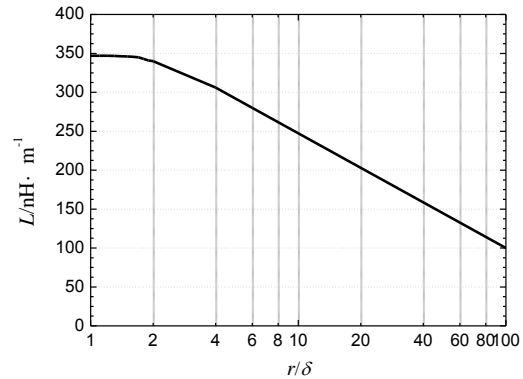


Fig. 8. Frequency dependency of inductance parameter expressed by the ratio of radius to skin depth.

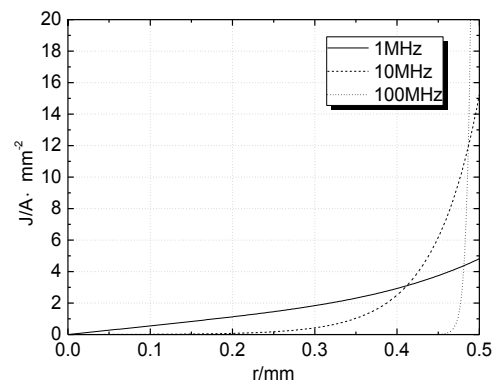


Fig. 9. Current distribution within the cross section of uniform transmission line at different frequency.

### B. Nonuniform transmission line model in free space

For better investigation of accuracy and availability of proposed method, the nonuniform transmission line model introduced in Fig. 1 is used in this section. The medium is free space. The two kind of different radius of signal line we used here are  $r_3=0.5-0.1(z/l)$  mm and  $r_4=0.5-0.05(z/l)$ . The size of ground plate and distance between signal line and ground plate are the same to Fig. 4. The length of signal line is 3000 mm, namely that coordinate  $z$  is from 0 to 3000 mm. New method and traditional method are used to solve the inductance parameter of this model.

Table 2 shows the filament numbers and computing time of the new method to calculate the inductance parameter in various frequency.

Table 2: Filament numbers and computing time in various frequency

$f/\text{MHz}$	$N_C$	$N_D$	$N_{\text{tot}}$	$t/\text{s}$
10	419	871	1290	0.6
100	1327	2972	4299	2.71
1000	4196	9615	13811	31.72

Figure 10 shows the inductance distribution of nonuniform transmission line in free space and 100 MHz frequency, which indicates that the unit inductance parameter is gradually increased with the increased coordinate  $z$ . So we can conclude that the unit inductance parameter of nonuniform transmission line in free space is increased with the decreased radius when the frequency of current is constant. Moreover, the traditional method has been used to prove the validity of the proposed method [17]. In the traditional method, the nonuniform transmission lines are considered to be equivalent to a cascaded chain of many multiport subnetworks which are made of short sections of uniform lines. Compare the two methods, the changing trend of the new method is more pronounced than the traditional one.

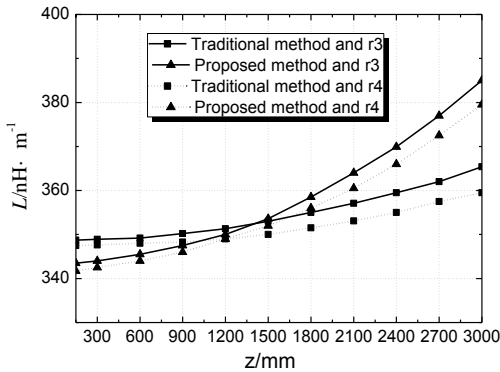


Fig. 10. Inductance distribution of nonuniform transmission line in free space.

For analysis of frequency dependency of unit inductance parameter of nonuniform transmission line in

free space, the unit line in  $z=150$  mm is calculated. The result is shown in Fig. 11, which indicates the unit inductance parameter is decreased with the increased frequency. It is caused by skin effect, which makes the current distribute near the surface of line so that the effective section can be decreased. Besides, when the frequency is 0.1 GHz, the inductance value in Fig. 10 is 344nH/m, which also is the value corresponding to  $z=150$  mm in Fig. 10.

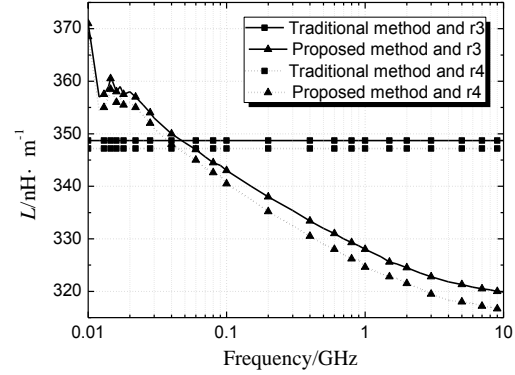


Fig. 11. Frequency dependency of inductance parameter for nonuniform transmission line in free space.

### C. Nonuniform transmission line model in anisotropic dielectric

Because the traditional method cannot solve the inductance parameter of nonuniform transmission line in anisotropic dielectric, in this section, the new method is applied to calculating the model of Fig. 1. The anisotropic dielectric we choose here is the uniaxial anisotropic medium, which is widely used in the microwave field of aviation industry. In this paper, we take the two kind of anisotropic dielectric as the example to analyze the influence of anisotropic dielectric on the inductance parameters. The tensor dielectric constant of anisotropic dielectric 1 is  $\epsilon_{11}=1.44\epsilon_0$ ,  $\epsilon_{22}=1.12\epsilon_0$ ,  $\epsilon_{33}=1.44\epsilon_0$ , and the tensor dielectric constant of anisotropic dielectric 2 is  $\epsilon_{11}=2.88\epsilon_0$ ,  $\epsilon_{22}=2.24\epsilon_0$ ,  $\epsilon_{33}=2.88\epsilon_0$ .

Table 3 shows the filament numbers and computing time of the new method to calculate inductance parameter in various frequency. Comparing the data in Table 3 with Table 2, we can conclude that the computing time of the model in anisotropic dielectric is longer than in free space. That is caused by the tensor dielectric constant with three-degree matrix, which leads to a more complex matrix processing process and increased computing time.

Table 3: Filament numbers and computing time in various frequency

$f/\text{MHz}$	$N_C$	$N_D$	$N_{\text{tot}}$	$t/\text{s}$
10	419	871	1290	0.9
100	1327	2972	4299	3.12
1000	4196	9615	13811	39.72

Figure 12 is the inductance distribution of nonuniform transmission line in different medium and 100 MHz frequency. The figure shows the inductance parameter increases with the decrease of transmission line's radius. Compared with Fig. 10, the value in Fig. 12 is bigger than in Fig. 10, which is caused by the principal axis of tensor dielectric constant. Besides, the isotropic dielectric of  $\epsilon=1.44\epsilon_0$  is compared with the anisotropic medium. It shows the inductance parameter is reduced in anisotropic dielectric when other conditions are the same. Because both the real part and the imaginary part of the magnetic field intensity are reduced in anisotropic dielectric. And it can decrease with the increase of coefficient of tensor dielectric constant.

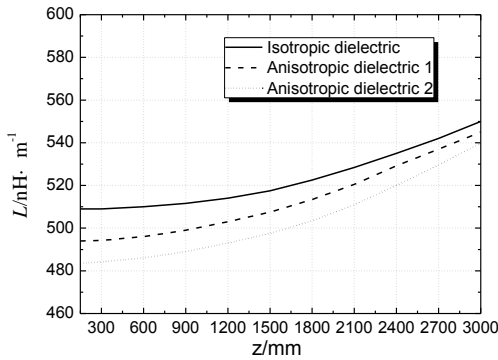


Fig. 12. Inductance distribution of nonuniform transmission line in different medium and 100 MHz.

For better analysis of new method, the frequency dependency of unit inductance parameter for nonuniform transmission line model in anisotropic dielectric is solved. The process of simulation is the same to Fig. 11 and shown in Fig. 13. It indicates that the inductance parameter is decreased with frequency. And when frequency is more than 1 GHz, the unit inductance parameter is decreased in exponential form. Therefore, anisotropic dielectric has a great influence on inductance parameter, and it should not be ignored in solving electric parameter of transmission line.

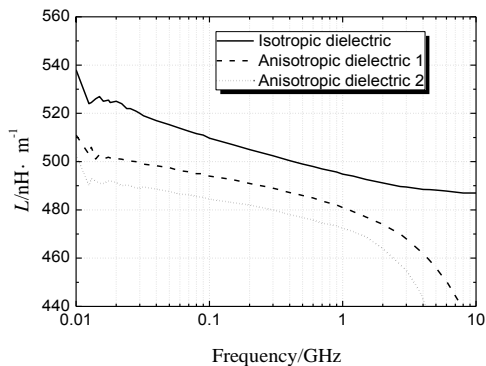


Fig. 13. Frequency dependency of inductance parameter for nonuniform transmission line in different dielectric.

## V. CONCLUSION

A novel method has been proposed for extracting inductance parameter of nonuniform transmission line in anisotropic dielectric. The proposed method can take the nonuniform distributed resistance and current caused by skin effect in high frequency and complex form of tensor dielectric constant into consideration. The correctness, validation, and accuracy of proposed method are demonstrated by several examples. The results show that the new method can be applied to solving inductance parameter when the model medium is anisotropic dielectric and transmission line is nonuniform. Moreover, it can be applied to solving various nonuniform transmission line structures and different anisotropic dielectric conditions.

## ACKNOWLEDGMENT

This project was supported by the National Natural Science Foundation of China (Grant No. 51209055), the China Postdoctoral Special Foundation (Grant No. 2015T80324), and the Natural Science Foundation of Heilongjiang, China (Grant No. F2015028).

## REFERENCES

- [1] D. Lei and D. Jiao, "Sensitivity analysis of lossy nonuniform transmission lines with nonlinear terminations," *IEEE Trans. Adv. Packag.*, vol. 33, no. 2, pp. 492-497, May 2010.
- [2] T. Takahiro, S. Tadatoshi, and A. Hideki, "Fast transient analysis of nonuniform multiconductor transmission lines using HIE-Block-LIM," *IEEE Microw. Wirel. Co.*, vol. 23, no. 10, pp. 512-514, Oct. 2013.
- [3] L. Jacek, "Equivalent circuits for nonuniform transmission line simulation," *Applied Comput. Electromagn. Society J.*, vol. 25, no. 9, pp. 764-779, Sep. 2010.
- [4] Q. Xu and P. Mazumder, "Accurate modeling of lossy nonuniform transmission lines by using differential quadrature methods," *IEEE Trans. Microw. Theory Tech.*, vol. 50, no. 10, pp. 2233-2246, Oct. 2002.
- [5] K. Afrooz and A. Abdipour, "Efficient method for time-domain analysis of lossy nonuniform multiconductor transmission line driven by a modulated signal using FDTD technique," *IEEE Trans. Electromagn. Compat.*, vol. 54, no. 2, pp. 482-494, Apr. 2012.
- [6] V. Nayyeri, M. Soleimani, and O. M. Ramahi, "A method to model thin conductive layers in the Finite-Difference Time-Domain method," *IEEE Trans. Electromagn. Compat.*, vol. 56, no. 2, pp. 385-392, Apr. 2014.
- [7] Y. Liu, J. Hong, and K. K. Mei, "Analysis of a double step microstrip discontinuity using generalized transmission line equations," *IEEE*

- Trans. Adv. Packag.*, vol. 26, no. 4, pp. 368-374, Nov. 2003.
- [8] C. R. Paul and A. E. Feather, "Computation of the transmission line inductance and capacitance matrices from the generalized capacitance matrix," *IEEE Trans. Electromagn. Compat.*, vol. 18, no. 4, pp. 175-183, Dec. 1976.
- [9] Y. Altuncu, "A numerical method for electromagnetic scattering by 3-D dielectric objects buried under 2-D locally rough surfaces," *IEEE Trans. Antennas Propagat.*, vol. 63, no. 8, pp. 3634-3643, Aug. 2015.
- [10] M. Kamon, M. J. Tsuk, and J. White, "FastHenry: A multipole-accelerated 3-D inductance extraction program," *IEEE Trans. Microw. Theory Tech.*, vol. 42, no. 9, pp. 1750-1758, Sep. 1994.
- [11] Y. Li, J. Li, and M. Wang, "Internal and external electric field for an anisotropic dielectric particle in electromagnetic beams," *IEEE Trans. Antennas Propagat.*, vol. 61, no. 9, pp. 4754-4759, 2013.
- [12] K. Agarwal, P. Li, and X. Chen, "Subspace-based optimization method for reconstruction of 2-D complex anisotropic dielectric objects," *IEEE Trans. Microw. Theory Tech.*, vol. 58, no. 4, pp. 1065-1074, Apr. 2010.
- [13] B. Carl, W. Gregory, and C. John, "A second-order 2D electromagnetics algorithm for curved interfaces between anisotropic dielectrics on a Yee mesh," *J. Comput. Phys.*, no. 230, pp. 2060-2075, 2011.
- [14] S. N. Dudorov, D. V. Lioubtchenko, and A. V. Raisanen, "Modification of marcatili's method for the calculation of anisotropic dielectric waveguides," *IEEE Trans. Microw. Theory Tech.*, vol. 50, no. 6, pp. 1640-1642, June 2002.
- [15] B. Benjamin, R. David, and N. Robert, "Multi-conductor spectral domain analysis of the mutual coupling between printed dipoles embedded in stratified uniaxial anisotropic dielectrics," *IEEE Trans. Antennas Propagat.*, vol. 60, no. 4, pp. 1886-1898, Apr. 2012.
- [16] C. R. Paul and A. E. Feather, "Computation of the transmission line inductance and capacitance matrices from the generalized capacitance matrix," *IEEE Trans. Electromagn. Compat.*, vol. 18, no. 4, pp. 175-183, 1976.
- [17] J. Mao and Z. Li, "Analysis of the time response of nonuniform multiconductor transmission lines with a method of equivalent cascaded network chain," *IEEE Trans. Microw. Theory Tech.*, vol. 40, no. 5, pp. 948-954, May 1992.